Glycoconjugate Journal (2022) 39:315–325
https://doi.org/10.1007/s10719-021-10018-8

ORIGINAL ARTICLE

Structural characteristics of Heparan sulfate required for the binding with the virus processing Enzyme Furin

Jiaxin Zeng[1,2,4] · Yuan Meng[2] · Shi-Yi Chen[2,3,4] · Gaofeng Zhao[2,4] · Lianchun Wang[5] · En-Xin Zhang[1] · Hong Qiu[2,3,4]

Received: 13 May 2021 / Revised: 8 July 2021 / Accepted: 7 August 2021 / Published online: 26 October 2021

Abstract

Furin is one of the nine-member proprotein convertase family. Furin cleaves proteins with polybasic residues, which includes many viral glycoproteins such as SARS-Cov-2 spike protein. The cleavage is required for the activation of the proteins. Currently, the mechanisms that regulate Furin activity remain largely unknown. Here we demonstrated that Furin is a novel heparin/heparan sulfate binding protein by the use of biochemical and genetic assays. The K_D is 9.78 nM based on the bio-layer interferometry assay. Moreover, we found that sulfation degree, site-specific sulfation (N-sulfation and 3-O-sulfation), and iduronic acid are the major structural determinants for the binding. Furthermore, we found that heparin inhibits the enzymatic activity of Furin when pre-mixes heparin with either Furin or Furin substrate. We also found that the Furin binds with cells of different origin and the binding with the cells of lung origin is the strongest one. These data could advance our understanding of the working mechanism of Furin and will benefit the Furin based drug discovery such as inhibitors targeting the interaction between heparan sulfate and Furin for inhibition of viral infection.

Keywords Furin · Heparan sulfate · Heparin · Virus infection · Carbohydrate-protein interaction

Introduction

Furin is the first member identified in the nine-member proprotein convertase family [1]. Furin ubiquitously cleaves proteins with polybasic residues such as cytokines, growth factors, hormones, and receptors in mammalian cells and is involved in different diseases such as cancer [2]. The Furin cleavage is also essential for viral glycoproteins to gain fusogenic activity. The Furin cleavage site RXR/KR is ubiquitously expressed in different viral glycoproteins such as the human immunodeficiency virus-1 (HIV-1) gp160 [3], Zika virus glycoprotein [4], Ebola virus prM [5], Influenza virus hemagglutinin [6], and the causative virus for COVID-19-SARS-CoV-2 spike protein [7], etc. After Furin cleavage, the viruses fuse with the host cell membrane and enter the host cell to initiate their replication. Based on these discoveries, Furin emerges as a potential target for the anti-viral drug development.

Although Furin cleavage is required for virus infection, the mechanisms that regulate Furin-mediated cleavage remain largely unknown. The proprotein convertase subtilisin kexin 9 (PCSK9) in the proprotein convertase family was reported to be a heparan sulfate binding protein, and the binding is critical for the degradation of low-density lipid receptor (LDLR) [8]. Moreover, the Furin cleavage site RXR/KR is a typical heparin/heparan sulfate binding motif. PC5B and PACE4 bind with heparan sulfate through their cysteine-rich domain [9] and Furin has a cysteine-rich domain as well. The binding of heparin to gp160 peptides including REKR and KAKR facilitates

✉ En-Xin Zhang
ergep53@126.com

✉ Hong Qiu
hongqiu@simm.ac.cn

1 The First Affiliated Hospital of Guangzhou University of Chinese Medicine, No. 16 Jichang Road, Guangdong Province 510405 Guangzhou, China

2 Carbohydrate-Based Drug Research Center, Shanghai Institute of Materia Medica, Chinese Academy of Sciences, 555 Zuchongzhi Road, Shanghai 200031, China

3 Nanjing University of Chinese Medicine, 138 Xianlin Road, Nanjing 210023, China

4 School of Pharmacy, University of Chinese Academy of Sciences, No. 19A Yuquan Road, Beijing 100049, China

5 Department of Molecular Pharmacology and Physiology, Morsani College of Medicine, University of South Florida Health, Tampa, FL, USA

the cutting of the peptide by Furin [10]. Moreover, there are several heparin/heparan sulfate binding motifs in the Furin sequence (supplemental information S1). Inspired by these facts, we hypothesize that the Furin is also a heparin/heparan sulfate binding protein. The most recent discovery by ourselves and other groups that cell surface heparan sulfate is a potential co-receptor for SARS-CoV-2 infection further stimulates us to test the hypothesis [11–14].

In this research, we first performed ELISA assay with heparin compound and the murine lung endothelial cells with heparan sulfate depleted, and the results clearly shown that Furin is a novel heparin/heparan sulfate binding protein. We further found that sulfation degree, N-sulfate, 3-O-sulfate, and iduronic acid are major determinants for the Furin binding. The K_D is determined to be 9.78 nM by biolayer interferometry analysis. Heparin inhibits the enzymatic activity of Furin when pre-mixes heparin with either Furin or Furin substrate. The Furin ubiquitously binds with cells of different origin and the binding to the cells of lung origin is the highest among the cells tested.

Materials and methods

Materials

Biotinylated-heparin (375054, 15 kDa) was purchased from EMD Millipore (USA). The heparin (Hep), 2-O-desulfated heparin (2DS), 6-O-desulfated heparin (6DS), N-desulfated heparin (NDS), completely desulfated heparin (CDS), and completely desulfated re N-sulfated Heparin (CDSNS) were all bought from GlycoNovo (Shanghai, China). K5 polysaccharide (K5), epimerized completely N-sulfated K5 polysaccharide (ENSK5), completely N, O-sulfated K5 polysaccharide (CNOSK5), completely N-sulfated K5 polysaccharide (CNSK5), N-deacetylated K5 polysaccharide (NDAK5), and completely N-deacetylated K5 polysaccharide (CNDAK5) are all obtained from GlycoNovo. N-Acetylneuraminic acid (Neu5Ac, A100555) and hyaluronic acid (HA, H107141) were obtained from Aladdin (Shanghai, China). Chondroitin sulfate A (CSA, YC1658691901) and chondroitin sulfate C (CSC, YC314581901) were bought from Carbosynth (United Kingdom). The surfen (S6951), chondroitinase ABC (C2905), and heparinase I, II, III (H2519, H6512, H8891) were sigma products. Recombinant human Furin with His tag is product from Acro Biosystems (Cat.# FUN-H5221, Lot.# 321-728F1-RS). The anti-His antibody conjugated with HRP was bought from ZENBIO (618194). All other reagents are from Sinopharm Chemical Reagent Co., Ltd. (Shanghai, China) if not specified.

Cells and cell culture

The murine lung endothelial cell (MLEC) lines were as previously reported[15].

The cell lines U87, SH-SY5Y, A549, MRC-5, WI-38, HuH-7, SK-HEP-1, Hep3B2.1–7, HT1080, EA.hy926, and HEK293 are ordered from National Collection of Authenticated Cell Cultures (Shanghai, China). All cells were cultured in medium supplemented with 10% fetal bovine serum (Gibco, 10099141C), 100 U/ml penicillin and 100 µg/ml streptomycin (Invitrogen, USA).

Enzyme-linked immunosorbent assay (ELISA) with immobilized Furin

Recombinant human Furin with His tag (100 µl) at 2.5 µg/ml were coated onto Immuno transparent flat 96 well plate with hydrophilic surface (Thermo, 439454) at RT for 2 h. Wash three times with 1 × PBS, each time 5 min. The plates were blocked with 3% BSA in 1 × PBS for 1 h at RT. After removing the blocking buffer, biotinylated heparin (1000, 500, 250, 125, 62.5, 31.25, 15.625 µg/ml) was added into the plate in 100 µl and incubated at RT for 1 h, the PBS serves as control. Pierce™ High Sensitivity Streptavidin-HRP (50 ng/ml, Thermo, 21132) was added and incubated for 1 h at RT. Wash with 1 × PBS 6 times. TMB (100 µl, Thermo, UJ2859123) was added and incubated at RT for 30 min. The reaction was stopped by adding 2 M H_2SO_4. The results were read by a spectrometer SpectraMax M5e (Molecular Devices, USA) at 450 nm.

Cell surface glycan processing

Cells (3.0×10^4 cells/well) were seeded into 96-well plates and cultured overnight. After washing with 1 × PBS, surfen (20 µM), chondroitinase ABC (5 U/ml) or heparinase I, II, III (4 U/ml, 0.5 U/ml, 0.5 U/ml) were added and incubated for 30 min, respectively. After the treatment, the digestion buffer was removed and the cells were washed with 1 × PBS for 3 times and fixed with 4% paraformaldehyde at room temperature (RT) for 15 min. The fixed cells were subject to cell-based enzyme-linked immunosorbent assay (ELISA) according to the following protocol.

Cell-based enzyme-linked immunosorbent assay (ELISA)

Cells (3.0×10^4 cells/well) were seeded into 96-well plates and incubated overnight at 37 ºC with 5% CO_2 in a humidified incubator. The cells were washed by 1 × PBS and then

fixed in 4% paraformaldehyde at room temperature (RT) for 15 min. After washed by 1 × PBS for 3 times, the cells were blocked in 3% BSA at RT for 90 min. After removing the blocking buffer, human Furin at 2.5 µg/ml or Furin-heparin mixture with Furin (2.5 µg/ml) and heparin (500 µg/ml) pre-mixed on ice for 30 min was added and incubated at RT for 1 h. The blank served as the control. The cells were washed 3 times with 1 × PBS and incubated with anti-His antibody conjugated with HRP (ZENBIO, 618194, 1:2000) for 1 h at RT. After 6 times washing with 1 × PBS, TMB (Thermo, UJ2859123) was added and incubated at RT for 30 min, the color development was stopped by 2 M H_2SO_4. Absorbance at 450 nm was measured by SpectraMax M5e (Molecular Devices, USA).

Carbohydrate-Based Enzyme-Linked Immunosorbent Assay (ELISA)

Carbohydrates (100 µl) in different concentration (1000, 500, 250, 125, 62.5, 31.25, 15.625 µg/ml) were coated into Immuno transparent flat 96 well plates with hydrophilic surface (Thermo, 439454) at RT for 2 h. Wash three times with 1 × PBS, each time 5 min. The plates were blocked with 3% BSA for 1 h at RT. Human Furin was added into the plates (0.25 µg/well in 100 µl 1 × PBS) after aspirating the blocking buffer and incubated at RT for 1 h. After 3 times washing by PBS, anti-His antibody conjugated with HRP (1:2000) was added and incubated for 1 h at RT. Wash with 1 × PBS 6 times. TMB (Thermo, UJ2859123) was added and incubated at RT for 30 min. The reaction was stopped by adding 2 M H_2SO_4. The absorbance of the developed substrate was read by a spectrometer SpectraMax M5e (Molecular Devices, USA) at 450 nm.

Biolayer interferometry assay

The Octet RED96 system (ForteBio, Menlo Park, CA) was used to determine the binding kinetics of the human furin to biotinylated-heparin (Millipore, 3532397) by immobilizing biotinylated-heparin onto Streptavidin (SA) coated sensors (ForteBio, 2105009911). The biotinylated-heparin (1 µg/ml in PBS) was loaded until the response unit (RU) reached 0.2 nm and enter the plateau state. Human Furin (650.4, 325.2, 162.6, 81.3, 40.7, 20.3, 10.2 nM) in PBST (PBS with 0.05% Tween20) was associated to sensor for 130 s and dissociated with PBST for 300 s. The biosensors were subsequently regenerated with 50 mM glycine solutin (pH = 1.7) (15 s) and PBST (15 s) for 5 times. The ForteBio Octet analysis software (ForteBio, Menlo Park, CA) was used to analyze the results. Association and dissociation rates were simultaneously fit to 1:1 ligand binding model to determine the affinity constant (K_D) value.

Flow cytometry analysis

Cells were collected after dissociation with PBS supplemented with 2 mM EDTA and 1% BSA (PBS-EB), and adjusted at 10^7 cells/ml. For Furin binding, the cells were incubated with 100 µl 2.5 µg/ml Furin on ice for 1 h. Following, the cells were incubated with SureLight® APC Anti-6X His tag® antibody (ABCAM, ab72579) on ice for 30 min, and were then subjected to flow cytometry analysis (CytoFLEX S, Beckman Coulter). The SureLight® APC conjugated isotype control (ABCAM, ab73711) serves as negative staining control. The results were analysed by FlowJo, and median fluorescence intensity (MFI) was calculated and presented.

Furin activity assay

Prepare assay buffer containing 25 mM Tris, 1 mM $CaCl_2$, 0.5% (w/v) Brij-35, pH 9.0. Dissolve the human Furin (Acro, FUN H52H3) and Furin substrate (Apeptide, APG1774) into assay buffer to form 2 µg/ml and 100 µM working solution, respectively. Heparin (GlycoNovo, C-HEPPIM) at 12.5 or 125 µg/ml were pre-mixed with either Furin or Furin substrate at 4 ºC for 30 min in 1:1 (v/v) ratio. Load the mixture (50 µl/well) into 96-well black plate (CORNING, 3925), initiate the reaction by adding substrate (50 µl/well) or furin (50 µl/well) at 37 ºC, let it react for 60 min. The Furin only or Furin substrate only group serves as negative control. The results were read by BioTek SYNERGY H1 microplate reader (BioTek Instruments Inc., Winooski, VT, USA) with excitation at 380 nm and emission at 460 nm.

Statistical analysis

All statistical analysis was performed by paired two-tail student's test, $p < 0.05$ was set to be of statistical significance. The data are presented as Mean ± SD, ns indicates not significant, * indicates $p < 0.05$, ** indicates $p < 0.01$, *** indicates $p < 0.001$. The GraphPad Prism v8.0.2.263 was used for most of the data analysis.

Results and discussion

Furin is a novel heparan sulfate binding protein

There are many methods can be used to characterize the interaction between glycans and their binding proteins [16]. We first chosen the ELISA to determine the binding affinity

of heparin to Furin. As shown in Fig. 1a, the binding affinity in the form of half maximal effective concentration (EC_{50}) of heparin to immobilized Furin is about 351.5 µg/ml or 23.4 µM. (Fig. 1b). We also determined the binding kinetics using the Octet RED96 system and the K_D was calculated to be 9.78 nM (Fig. 1b). Consistently, when we pre-mixed Furin with heparin and added the mixture onto the wild type murine lung endothelial cells (MLECs), we found that the binding of Furin to the cells was significantly blocked compared to the Furin and blank group (Fig. 1c). To further confirm the results, we performed cell-based ELISA using the murine lung endothelial cells (MLECs) with Ext1 deletion ($Ext1^{-/-}$) which is completely absent of heparan sulfate (HS) expression [15]. Compared to the wild type cells, the binding of Furin to the heparan sulfate depleted cells was reduced by nearly 50% (Fig. 1d). Surfen is a small molecule inhibitor for heparan sulfate [17], the binding of Furin to the immobilized cells was reduced by 36% when we treat the cells 30 min before we add the Furin protein (Fig. 1d). Heparinase I, II, III (HSase) treatment can digest the cell surface HS. Compared to the control, the binding of Furin was reduced by 46% after HSase treatment, while chondroitinase ABC

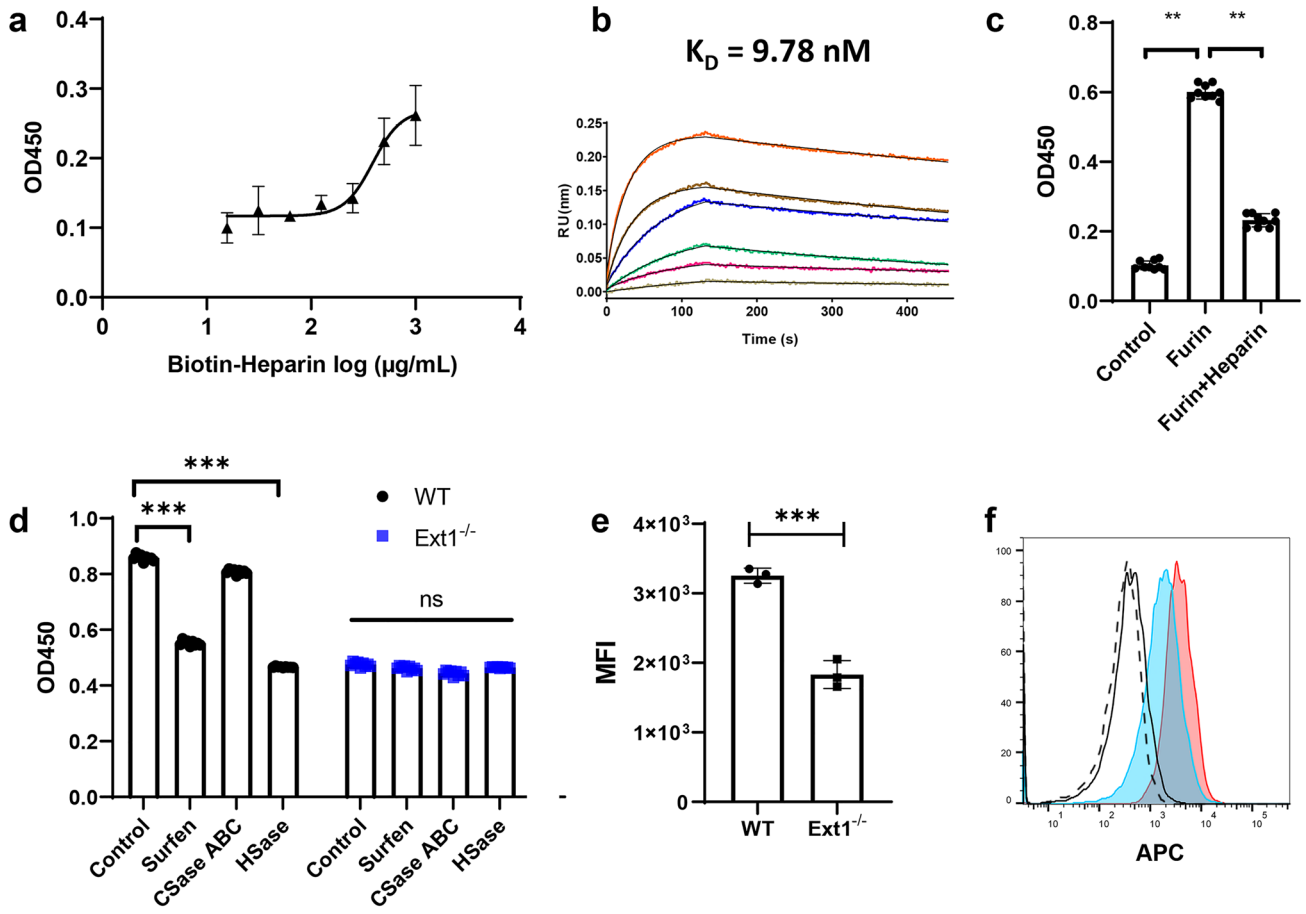

Fig.1 Furin is a novel heparin/heparan sulfate binding protein. The binding affinity of biotinylated-heparin to immobilized Furin is about 351.5 µg/ml or 23.4 µM based on ELISA **a**. The binding of Furin to biotinylated-heparin immobilized onto the streptavidin-based probe is determined by biolayer interferometry (BLI) and the K_D value is 9.78 nM. The concentration of Furin is 10.2, 20.3, 40.7, 81.3, 325.2, and 650.4 nM **b**. The binding of Furin or pre-mixture of Furin and heparin (Hep) to murine wild type lung endothelial cells based on cell-based ELISA, the cells without incubation with Furin served as control **c**. The binding of Furin to murine lung endothelial cells (MLECs) with heparan sulfate (HS) depleted ($Ext1^{-/-}$ cells) is significantly reduced by about 50% compared to the wild type cells as determined by cell-based ELISA. Heparan sulfate inhibitor surfen (20 µM) or heparinase I, II, and III (HSase, 4 U/ml, 0.5 U/ml, 0.5 U/ml), but not by chondroitinase ABC (CSase ABC, 5 U/ml) treatment at RT for 30 min impairs the binding of Furin to wild type murine lung endothelial cells, the cells without treatment serves as control **d**. Based on flow cytometry analysis, the binding of Furin to cell surface HS is significantly reduced in the HS depleted cells ($Ext1^{-/-}$cells) as the APC median fluorescence intensity (MFI) by anti-His antibody conjugated with APC is significantly reduced **e**. The bold line and dash line are isotype control for wild type cells and $Ext1^{-/-}$ cells, respectively; the red and cyan are wild type cells and $Ext1^{-/-}$cells, respectively **f**. Absorbance at 450 nm (OD450) is the indicative of binding capacity. Data are presented as Mean ± SD, ns indicates not significant, * indicates $p < 0.05$, ** indicates $p < 0.01$, *** indicates $p < 0.001$

(CSase ABC) treatment did not significantly alter the binding of Furin to the cells. Moreover, none of the treatment on the Ext1$^{-/-}$ cells leads to change in the binding of Furin to Ext1$^{-/-}$ cells (Fig. 1d).

We also measured the binding of Furin to wild type and Ext1$^{-/-}$ murine lung endothelial cells (MLECs) by the flow cytometry. Consistent with the aforementioned results, the binding of Furin to Ext1$^{-/-}$ cells determined by median fluorescence intensity (MFI) was also significantly reduced by about 50% (Fig. 1e, f).

In all, we have shown that Furin is a novel heparin/heparan sulfate binding protein.

N- sulfate, 3-O- sulfate, and iduronic acid are major structural determinants required for heparan sulfate to bind Furin

Next, we sought to determine the structural characteristics of heparan sulfate for Furin binding. To do this, we performed cell-based ELISA using our recently developed heparan sulfate mutant cell library [15]. The binding of Furin to Ndst1$^{-/-}$, Ndst2$^{-/-}$, and Ndst1/2$^{-/-}$ cells was reduced by 24.8%, 36%, and 69%, respectively (Fig. 2a). As we previously reported, the sulfate degree, N-sulfate, and O-sulfate in the Ndst1$^{-/-}$, Ndst2$^{-/-}$, and Ndst1/2$^{-/-}$ cells are significantly reduced [15]. This shows that both site specific sulfation and sulfation degree are required for the binding of Furin. Epimerization of glucuronic acid is also required for the binding of Furin to heparan sulfate as the binding of Furin to Glce$^{-/-}$ cells is reduced by 24.1% (Fig. 2a). However, 2-O-sulfation is minimally required for the binding as the binding of Furin to the Hs2st$^{-/-}$ cells is only reduced by 3.7% when compared to the binding of Furin to the wild type cells (Fig. 2b). In our previous report, the 2-O-sulfate is reduced in the Glce$^{-/-}$ cells and disappeared in the Hs2st$^{-/-}$ cells [15]. In addition to reduction of 2-O-sulfate in the Glce$^{-/-}$ cells, the iduronic acid is also reduced as the Glce encodes enzyme catalyze the conversion of glucouronic acid to iduronic acid. The more reduction of the Furin binding we observed in the Glce$^{-/-}$ cells than in the Hs2st$^{-/-}$ cells could be due to the reduction of both 2-O-sulfate and iduronic acid. The binding of Furin to Hs6st1$^{-/-}$, Hs6st2$^{-/-}$, and Hs6st1/2$^{-/-}$ cells is reduced by 4.1%, 7.4%, and 4.6%, respectively (Fig. 2c). In contrast,

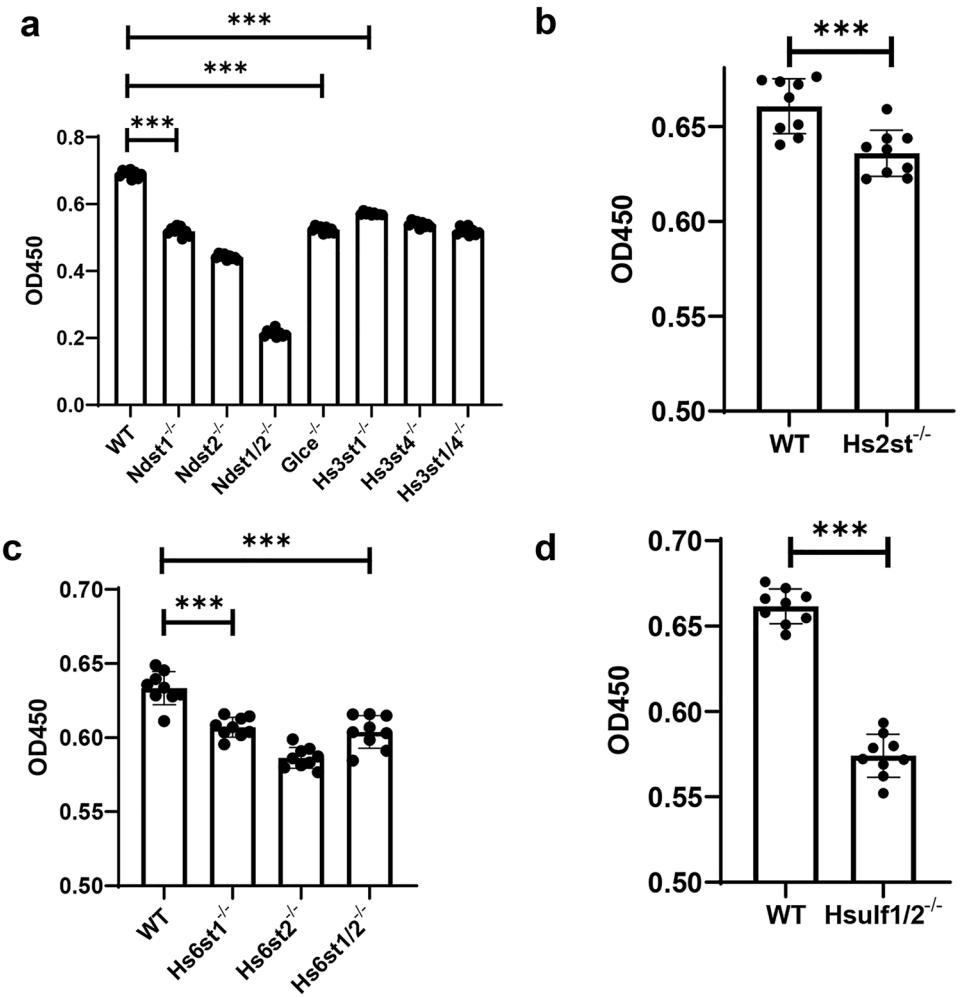

Fig. 2 Structural determinants in heparan sulfate for the binding of Furin to cell surface heparan sulfate determined by cell-based ELISA. As determined by cell-based ELISA, the binding of Furin to Ndst1$^{-/-}$, Ndst2$^{-/-}$, and Ndst1/2$^{-/-}$; Glce$^{-/-}$; Hs3st1$^{-/-}$, Hs3st4$^{-/-}$, and Hs3st1/4$^{-/-}$ cells are significantly reduced by 24.8%, 36%, 69%, 24.1%, 17.25%, 21.84%, and 24.73%, respectively **a**. The binding of Furin to Hs2st$^{-/-}$cells is reduced by 3.7% **b**. The binding of Furin to Hs6st1$^{-/-}$, Hs6st2$^{-/-}$, and Hs6st1/2$^{-/-}$ cells is reduced by 4.1%, 7.4%, and 4.6% **c**. The binding of Furin to Hsulf1/2$^{-/-}$ cells is reduced by 13.2% **d**. Absorbance at 450 nm (OD450) is the indicative of binding capacity. Data are presented as Mean ± SD, ns indicates not significant, * indicates $p < 0.05$, ** indicates $p < 0.01$, *** indicates $p < 0.001$

the binding of Furin to Hsulf1/2$^{-/-}$ cells is reduced by 13.2% compared to the wild type cells (Fig. 2d). As we previously reported, the 6-O-sulfate is reduced in Hs6st1/2$^{-/-}$ cells but increased in Hsulf1/2$^{-/-}$ cells when compared to wild type cells [15]. Meanwhile, the sulfate degree in both Hs6st1/2$^{-/-}$ cells and Hsulf1/2$^{-/-}$ cells are reduced compared to the wild type cells [15]. The reduction of binding to these two cell lines indicates that the binding of Furin to heparan sulfate is more dependent on the sulfate degree than the 6-O-sulfate. Compared to the wild type cells, the binding of Furin to Hs3st1$^{-/-}$, Hs3st4$^{-/-}$, and Hs3st1/4$^{-/-}$ cells is significantly reduced by 17.25%, 21.84%, and 24.73%, respectively (Fig. 2a). The HS3ST1 and HS3ST4 enzyme are required for the generation of 3-O-sulfate for the antithrombin III (ATIII) and glycoprotein D (gD) specific binding, respectively [18]. We have demonstrated that ATIII binding to Hs3st1$^{-/-}$, Hs3st4$^{-/-}$, and Hs3st1/4$^{-/-}$ cells are reduced, which indicates that ATIII specific binding 3-O-sulfate is reduced or disappeared in the knockout cells [15]. The sulfate degree in Hs3st4$^{-/-}$ cells is also reduced when compared to wild type cells, Hs3st1$^{-/-}$, and Hs3st1/4$^{-/-}$ cells [15]. The reduction of Furin binding is thus because of the reduction of 3-O-sulfate in Hs3st1$^{-/-}$ and Hs3st1/4$^{-/-}$ cells and the reduction of both 3-O-sulfate and sulfate degree in Hs3st4$^{-/-}$ cells.

These data show that the sulfation degree, N-sulfate, 2-O-sulfate, 6-O-sulfate, 3-O- sulfate, and iduronic acid are structural determinants in heparan sulfate for their binding with Furin. The contribution of N-sulfate, 3-O-sulfate, and iduronic acid is greater than others.

Heparin and heparin derivatives bind with Furin in different affinity

We have demonstrated that sulfation degree, N-sulfate, 2-O-sulfation, 6-O-sulfate, 3-O- sulfate, and iduronic acid are structural determinants for the binding of Furin to the cell surface heparan sulfate. We next try to explore the binding potential of heparin with different structure to the Furin protein. We use the ELISA to determine the binding of Furin to immobilized heparin (Hep), completely desulfated heparin (CDS), N-desulfated heparin (NDS), 2-O-desulfated heparin (2DS), 6-O-desulfated heparin (6DS), and completely desulfated N-resulfated heparin (CDSNS).

The completely de-sulfated heparin (CDS) almost loses its binding to Furin. The binding pattern of Furin to N-desulfated heparin (NDS) is similar to that of CDS, but N-re-sulfation of CDS (CDSNS) leads to an increase of binding of Furin with the polysaccharide. This indicates that N-sulfate is a critical determinant for the binding to Furin. Consistent with the binding to cell surface heparan sulfate, 2-O-desulfated heparin (2DS) shows the strongest binding to Furin among the modified heparins we tested. Furin also binds with the 6-O-desulfated heparin (6DS) but the binding affinity is lower than the binding with the 2DS. This shows that the contribution of 2-O-sulfate to the binding of Furin to heparin/heparan sulfate is less important than N-sulfation and 6-O-sulfation (Fig. 3a). According to the product information sheet, the sulfur content in Hep, CDS, NDS, CDSNS, 2DS, and 6DS is 11–14%, < 2%, 7–8.5%, 5.5–8.5%, 7.5–9.5%, and 7–9%, respectively (Supplemental Information S2-S8). The sulfur content in Hep is the highest among the polysaccharides tested. Intriguingly, the binding of Furin to Hep is the strongest among the polysaccharides tested as well. This shows that both sulfation degree and site-specific sulfation are required for the binding with Furin, which is consistent with the data based on heparan sulfate mutant cells.

Furin does not bind to Chondroitin sulfate, Hyaluronan (HA), and N-acetylneuraminic acid (Neu5Ac)

To further explore the selectivity of the binding of Furin to glycosaminoglycan and acidic carbohydrates, we determined the binding of Furin to the chondroitin sulfate A (CSA), chondroitin sulfate C (CSC), hyaluronan (HA), and N-acetylneuraminic acid (Neu5Ac) in the same conditions for heparin binding. The binding affinity of Furin to these carbohydrates is comparable to the completely de-sulfated heparin (Fig. 3b). These show that Furin only binds to sulfated polysaccharide with a specific backbone.

Furin does not bind with K5 polysaccharide but bind with sulfated derivatives of K5 polysaccharide

The Escherichia coli K5 capsular polysaccharide (K5) [-4)-βGlcA-(1,4)-αGlcNAc-(1-] is structurally similar to the non-sulfated heparin/heparan sulfate. Theoretically, the K5 sulfate derivatives might be used as competitive inhibitors for the binding between heparan sulfate and Furin. To test this hypothesis, we determined the binding of Furin to epimerized completely N-sulfated K5 polysaccharide (ENSK5), completely N, O-sulfated K5 polysaccharide (CNOSK5), completely N-sulfated K5 polysaccharide (CNSK5), N-deacetylated K5 Polysaccharide (NDAK5), and completely N-Deacetylated K5 polysaccharide (CNDAK5).

As expected, K5 polysaccharide shows almost no binding with Furin. N-deacetylation does not change the binding of K5 polysaccharide to Furin, as the binding pattern of Furin to NDAK5 and CNDAK5 is almost the same as the K5. Both N-sulfation (CNSK5) and completely N-, O- sulfation of K5 (CNOSK5) leads to a significant increase of binding to Furin (Fig. 3c). However, there is only a trace level binding of Furin to epimerized completely N-sulfated K5 polysaccharide (ENSK5). This could be due to the lower sulfation of ENSK5 compared to CNOSK5, as the sulfur content in

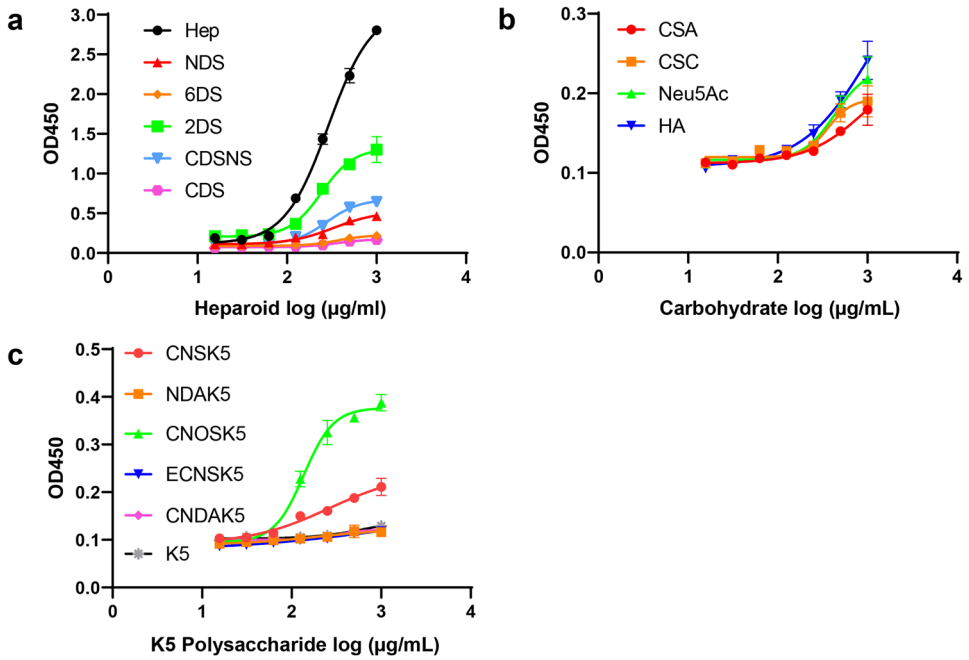

Fig. 3 The binding of Furin with different carbohydrates. **a** The binding of Furin to heparin (Hep), 2-O-desulfated heparin (2DS), 6-O-desulfated heparin (6DS), N-desulfated heparin (NDS), completely desulfated heparin (CDS), and completely desulfated re N-sulfated heparin (CDSNS) in different concentration (1000, 500, 250, 125, 62.5, 31.25, 15.625, 0 μg/ml) were determined by ELISA. **b** The binding of Furin to chondroitin sulfate A (CSA), chondroitin sulfate C (CSC), N-acetylneuraminic acid (Neu5Ac) in different concentration (1000, 500, 250, 125, 62.5, 31.25, 15.625, 0 μg/ml) were determined by ELISA. **c** The binding of Furin to K5 polysaccharide (K5), epimerized completely N-sulfated K5 polysaccharide (ENSK5), completely N, O-sulfated K5 polysaccharide (CNOSK5), completely N-sulfated K5 polysaccharide (CNSK5), N-deacetylated K5 Polysaccharide (NDAK5), and completely N-Deacetylated K5 polysaccharide (CNDAK5) in different concentration (1000, 500, 250, 125, 62.5, 31.25, 15.625, 0 μg/ml) were determined by ELISA. Absorbance at 450 nm (OD450) is the indicative of binding capacity. Data are presented as Mean ± SD, ns indicates not significant, * indicates $p < 0.05$, ** indicates $p < 0.01$, *** indicates $p < 0.001$

ENSK5 and CNOSK5 is 3–5% and 15–16.3%, respectively (Supplemental Information S2, S10 and S12). These results are also in consistent with our data based on heparan sulfate mutant cells and heparin and chemically modified heparin.

Furin binds to cells of different origin with different affinity in a heparan sulfate dependent way

Esko et al. have determined the structure of heparan sulfate from human lung, tonsil, kidney, and liver, and they found that sulfation degree, N-sulfate, and 2-O-sulfate is higher in lung tissue than in the other three tissues [13]. HS from human lung tissue shows the strongest inhibitory effect on the binding of SARS-Cov-2 spike protein receptor binding domain (RBD) to H1299 cells [13]. We have established that Furin is a new heparin/heparan sulfate binding protein. We next sought to determine the binding of Furin to cells of different origin, to see whether the interaction between heparin/heparan sulfate and Furin can be determinants for the viral tropism. We included cells of lung origin (A549, MRC-5, and WI-38), cells of liver origin (HuH-7, SK-HEP-1, and Hep3B2.1–7), cells of brain origin (U87 and SH-SY5Y), human umbilical vein endothelial cells EA.hy926, human fibrosarcoma cells HT1080, and human embryonic kidney cells HEK293. We found that Furin bind to the cells of lung origin with the highest affinity. The binding was diminished after the cells treated with heparinase I, II, and III (HSase) (Fig. 4a). The binding of heparin-Furin pre-mixture to the immobilized cells is also significantly reduced when compared to the binding of Furin to the immobilized cells (Fig. 4b). These evidences further confirmed that Furin is a heparin/heparan sulfate binding protein and the binding of Furin to the cells is dependent on the cell surface heparan sulfate and the binding affinity varies in different tissues.

Heparin inhibits the Furin enzymatic activity through binding either Furin or the Furin substrate

We next asked whether heparin could inhibit the enzymatic activity of Furin. Because heparin binds both Furin and Furin substrates, we hypothesize that heparin binding either Furin or Furin substrates blocks the Furin activity. To test the hypothesis, we pre-mixed the heparin with either Furin or Furin substrate at RT for 30 min before initiating

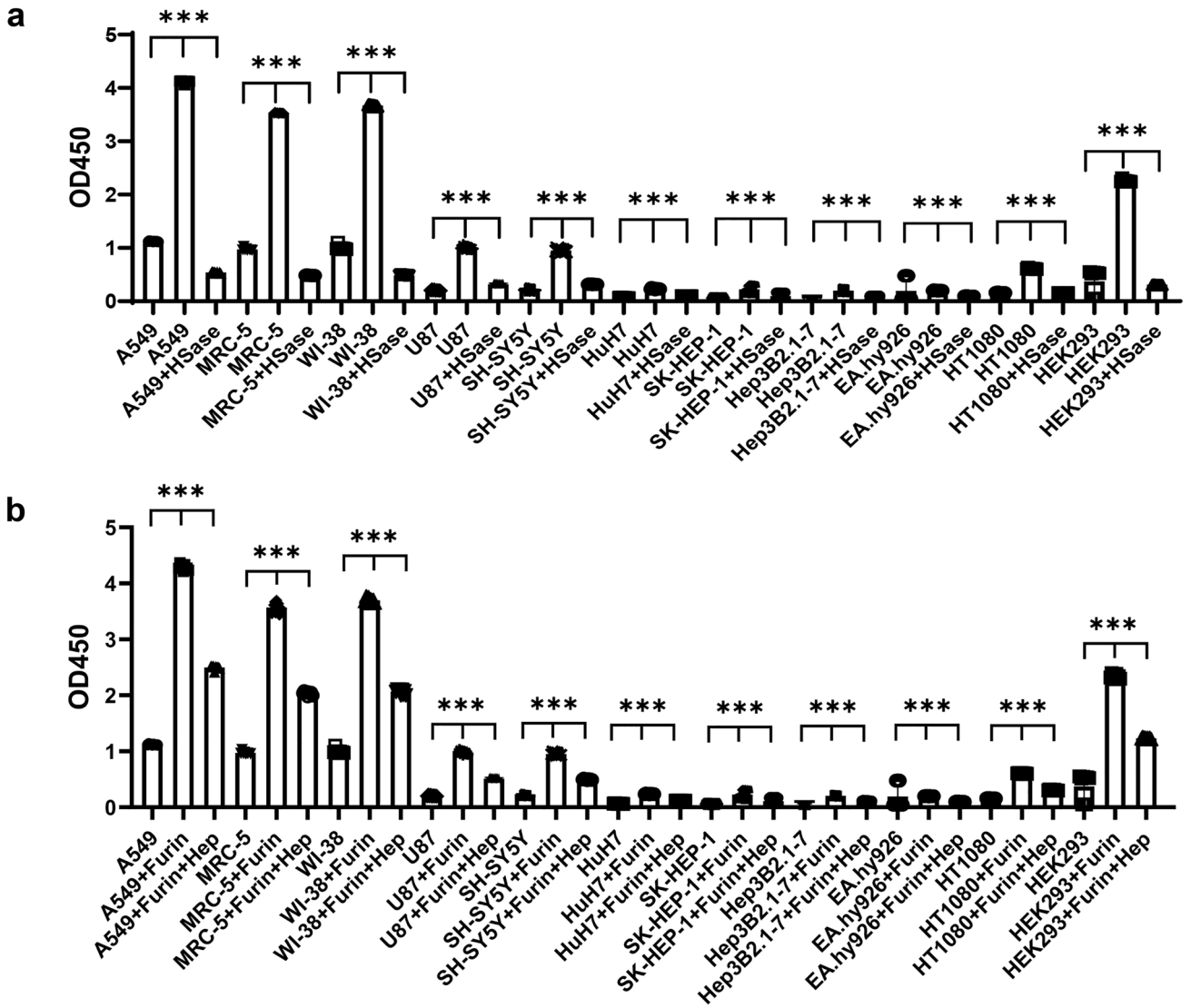

Fig. 4 Furin binds to cells of different origin in different affinity and the binding is heparan sulfate dependent. The cells of lung origin (A549, MRC-5, and WI-38), cells of liver origin (HuH-7, SK-HEP-1, and Hep3B2.1–7), cells of brain origin (U87 and SH-SY5Y), human umbilical vein endothelial cells EA.hy926, human fibrosarcoma cells HT1080, and human embryonic kidney cells HEK293 all bind with Furin and the binding to the cells of lung origin is the strongest among the cells tested **a**. The binding is diminished after heparinase I, II, III (HSase) pretreatment at RT 30 min **a**. Pre-mixing heparin (Hep, 500 µg/ml) and Furin (2.5 µg/ml) leads to reduction of the binding of Furin to the immobilized cells **b**. The cells without Furin incubation served as control. Absorbance at 450 nm (OD450) is the indicative of binding capacity. Data are presented as Mean ± SD, ns indicates not significant, * indicates $p < 0.05$, ** indicates $p < 0.01$, *** indicates $p < 0.001$

the reaction. As shown in Fig. 5, heparin significantly inhibits the Furin enzymatic activity by pre-mixing heparin with either Furin or Furin substrate and the reaction is very quick. The results is consistent with the results that heparin inhibits the activation of latent TGFß-1 by inhibiting the processing of latent TGFß-1 by Furin [19]. But heparin enhances the Furin cleavage of HIV-1 gp160 peptides in different length [10], the difference could be due to the reaction condition and enzymatic activity determination method is different from what we used.

Several clinical trials are undergoing to investigate the effect of heparin on hospitalized COVID-19 patients (www.clinicaltrials.gov) with coagulopathy [20, 21]. Unfractionated heparin and low-molecular weight heparin (LMWH), and sulfated polysaccharides from different sources have been reported to bind with SARS-CoV-2 spike protein [14, 22, 23]. Their inhibitory effect on SARS-CoV-2 infection has also been widely tested. These data suggest that heparin could also be used as prophylactic drug for SARS-CoV-2 infection [21].

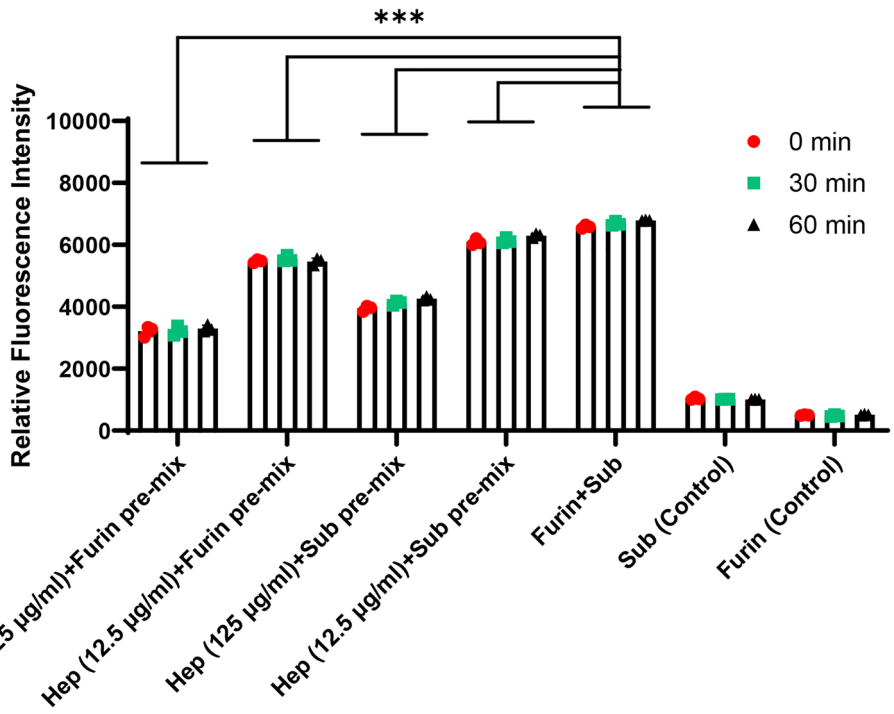

Fig. 5 The effect of heparin on the activity of Furin. Heparin (Hep, 12. 5 or 125 µg/ml) was pre-mixed with either Furin or Furin substrate (Sub) in 1:1 (v/v) ratio at 37 ℃ for 30 min. Load the mixture (50 µl/well) into 96-well black plate (CORNING, 3925), initiate the reaction by adding substrate (50 µl/well) or furin (50 µl/well) at 37 ℃ and let it react 60 min. The Furin only or Furin substrate only group serves as negative control. The results were read by BioTek SYNERGY H1 microplate reader (BioTek Instruments Inc., Winooski, VT, USA) with excitation at 380 nm and emission at 460 nm immediately, 30 min, or 60 min after initiating the reaction. Data are presented as Mean ± SD, ns indicates not significant, * indicates $p < 0.05$, ** indicates $p < 0.01$, *** indicates $p < 0.001$

Our results clearly shown that Furin is a novel heparin/heparan sulfate binding protein. Previous research has shown that SARS-CoV-2 spike protein is also heparin/heparan sulfate binding protein. In this scenario, heparan sulfate on the cell surface may serve as a scaffold which tether the related proteins together to facilitate their interaction and initiate the downstream biological events [24]. Put these together, we may get a clearer picture of how the heparan sulfate function during the SARS-CoV-2 infection and virus infection in general although the elucidation of the three-dimensional structure of the complex formed by heparan sulfate, Furin, and the SARS-Cov-2 spike protein is warranted. This may not be limited to virus infection but could be expanded to Furin cleavage related biological processes.

Recent study found that there is an increase of plasma level of Furin in patients with coronary artery disease and COVID-19, and the increase of the plasma level of Furin is independent prognostic factor for the progression of respiratory failure in the patients [25]. Our results here thus can explain why the increase of Furin in plasma leads to poor prognosis of the patients and provide further scientific support for the use of the approved heparin like drugs to treat patients with coronary artery disease and COVID-19.

Conclusion

Furin is a novel heparin/heparan sulfate binding protein and the binding is dependent on the sulfation degree, site specific sulfation (N- sulfate, 2-O-, 6-O-, 3-O- sulfate), and iduronic acid in the heparan sulfate. The results suggest that heparan sulfate may serve as a scaffold for the Furin to cleave its substrates and heparin could competitively block the function of heparan sulfate. This will not only advance our understanding of the effect of virus infection but also in other Furin cleavage related physiological and pathological processes. Moreover, our results provide support for the use of the approved heparin like drugs to treat patients with Furin-cleavage associated diseases such as patients with coronary artery disease and COVID-19.

Supplementary information The online version contains supplementary material available at https://doi.org/10.1007/s10719-021-10018-8.

Acknowledgements We thank for the start-up grant from "CAS Pioneer Talent Program" in Chinese Academy of Sciences and the support by Shanghai Pujiang Program (19PJ1411300).

Author contribution Hong Qiu conceived and supervised the research. Jiaxin Zeng, Yuan Meng, Shiyi Chen, Gaofeng Zhao, and Hong Qiu performed the study. Jiaxin Zeng, Yuan Meng, Shiyi Chen, Gaofeng Zhao, and Hong Qiu analyzed the data. Lianchun Wang provided the heparan sulfate deficient MLEC library. Hong Qiu wrote the manuscript and all the authors reviewed and approved the manuscript.

Funding Hong Qiu is supported by "CAS Pioneer Talent Program" in Chinese Academy of Sciences and the Shanghai Pujiang Program (19PJ1411300).

Availability of data and material Provided as Required.

Code availability Not Applicable.

Declarations

Ethics approval Not Applicable.

Consent to participate All authors agreed to participate.

Consent to publication All authors agreed to publish.

Conflict of interest/Competing interests Not Applicable.

References

1. Seidah, N.G., Prat, A.: The biology and therapeutic targeting of the proprotein convertases. Nat. Rev. Drug Discovery. **11**(5), 367–383 (2012). https://doi.org/10.1038/nrd3699
2. Braun, E., Sauter, D.: Furin-mediated protein processing in infectious diseases and cancer. Clin. Transl. Immunol. **8**(8), e1073 (2019). https://doi.org/10.1002/cti2.1073
3. Hallenberger, S., Bosch, V., Angliker, H., Shaw, E., Klenk, H.D., Garten, W.: Inhibition of furin-mediated cleavage activation of HIV-1 glycoprotein gpl60. Nature. **360**(6402), 358–361 (1992). https://doi.org/10.1038/360358a0
4. Owczarek, K., Chykunova, Y., Jassoy, C., Maksym, B., Rajfur, Z., Pyrc, K.: Zika virus: mapping and reprogramming the entry. Cell Commun. Signaling. **17**(1), 41 (2019). https://doi.org/10.1186/s12964-019-0349-z
5. Volchkov, V.E., Feldmann, H., Volchkova, V.A., Klenk, H.D.: Processing of the Ebola virus glycoprotein by the proprotein convertase furin. Proc. Natl. Acad. Sci. **95**(10), 5762–5767 (1998). https://doi.org/10.1073/pnas.95.10.5762
6. Stieneke-Gröber, A., Vey, M., Angliker, H., Shaw, E., Thomas, G., Roberts, C., Klenk, H.D., Garten, W.: Influenza virus hemagglutinin with multibasic cleavage site is activated by furin, a subtilisin-like endoprotease. EMBO J. **11**(7), 2407–2414 (1992). https://doi.org/10.1002/j.1460-2075.1992.tb05305.x
7. Papa, G., Mallery, D.L., Albecka, A., Welch, L.G., Cattin-Ortolá, J., Luptak, J., Paul, D., McMahon, H.T., Goodfellow, I.G., Carter, A., Munro, S., James, L.C.: Furin cleavage of SARS-CoV-2 Spike promotes but is not essential for infection and cell-cell fusion. PLoS Pathog. **17**(1), e1009246 (2021). https://doi.org/10.1371/journal.ppat.1009246
8. Gustafsen, C., Olsen, D., Vilstrup, J., Lund, S., Reinhardt, A., Wellner, N., Larsen, T., Andersen, C.B.F., Weyer, K., Li, J.-P., Seeberger, P.H., Thirup, S., Madsen, P., Glerup, S.: Heparan sulfate proteoglycans present PCSK9 to the LDL receptor. Nat. Commun. **8**(1), 503 (2017). https://doi.org/10.1038/s41467-017-00568-7
9. Tsuji, A., Sakurai, K., Kiyokage, E., Yamazaki, T., Koide, S., Toida, K., Ishimura, K., Matsuda, Y.: Secretory proprotein convertases PACE4 and PC6A are heparin-binding proteins which are localized in the extracellular matrix: Potential role of PACE4 in the activation of proproteins in the extracellular matrix. Biochim. Biophys. Acta Proteins Proteomet. **1645**(1), 95–104 (2003). https://doi.org/10.1016/S1570-9639(02)00532-0
10. Pasquato, A., Dettin, M., Basak, A., Gambaretto, R., Tonin, L., Seidah, N.G., Di Bello, C.: Heparin enhances the furin cleavage of HIV-1 gp160 peptides. FEBS Lett. **581**(30), 5807–5813 (2007). https://doi.org/10.1016/j.febslet.2007.11.050
11. Yue, J., Jin, W., Yang, H., Faulkner, J., Song, X., Qiu, H., Teng, M., Azadi, P., Zhang, F., Linhardt, R.J., Wang, L.: Heparan Sulfate Facilitates Spike Protein-mediated SARS-CoV-2 Host Cell Invasion and Contributes to Increased Infection of SARS-CoV-2 G614 Mutant and in Lung Cancer. Front. Mol. Biosci. (2021). https://doi.org/10.3389/fmolb.2021.649575
12. Mycroft-West, C.J., Su, D., Pagani, I., Rudd, T.R., Elli, S., Gandhi, N.S., Guimond, S.E., Miller, G.J., Meneghetti, M.C.Z., Nader, H.B., Li, Y., Nunes, Q.M., Procter, P., Mancini, N., Clementi, M., Bisio, A., Forsyth, N.R., Ferro, V., Turnbull, J.E., Guerrini, M., Fernig, D.G., Vicenzi, E., Yates, E.A., Lima, M.A., Skidmore, M.A.: Heparin Inhibits Cellular Invasion by SARS-CoV-2: Structural Dependence of the Interaction of the Spike S1 Receptor-Binding Domain with Heparin. Thromb Haemost. **120**(12), 1700–1715 (2020). https://doi.org/10.1055/s-0040-1721319
13. Clausen, T.M., Sandoval, D.R., Spliid, C.B., Pihl, J., Perrett, H.R., Painter, C.D., Narayanan, A., Majowicz, S.A., Kwong, E.M., McVicar, R.N., Thacker, B.E., Glass, C.A., Yang, Z., Torres, J.L., Golden, G.J., Bartels, P.L., Porell, R.N., Garretson, A.F., Laubach, L., Feldman, J., Yin, X., Pu, Y., Hauser, B.M., Caradonna, T.M., Kellman, B.P., Martino, C., Gordts, P.L.S.M., Chanda, S.K., Schmidt, A.G., Godula, K., Leibel, S.L., Jose, J., Corbett, K.D., Ward, A.B., Carlin, A.F., Esko, J.D.: SARS-CoV-2 Infection Depends on Cellular Heparan Sulfate and ACE2. Cell. **183**(4), 1043-1057.e1015 (2020). https://doi.org/10.1016/j.cell.2020.09.033
14. Kim, S.Y., Jin, W., Sood, A., Montgomery, D.W., Grant, O.C., Fuster, M.M., Fu, L., Dordick, J.S., Woods, R.J., Zhang, F., Linhardt, R.J.: Characterization of heparin and severe acute respiratory syndrome-related coronavirus 2 (SARS-CoV-2) spike glycoprotein binding interactions. Antiviral Res. **181**, 104873 (2020). https://doi.org/10.1016/j.antiviral.2020.104873
15. Qiu, H., Shi, S., Yue, J., Xin, M., Nairn, A.V., Lin, L., Liu, X., Li, G., Archer-Hartmann, S.A., Dela Rosa, M., Galizzi, M., Wang, S., Zhang, F., Azadi, P., van Kuppevelt, T.H., Cardoso, W.V., Kimata, K., Ai, X., Moremen, K.W., Esko, J.D., Linhardt, R.J., Wang, L.: A mutant-cell library for systematic analysis of heparan sulfate structure–function relationships. Nat. Methods. **15**(11), 889–899 (2018). https://doi.org/10.1038/s41592-018-0189-6
16. Cummings, R.D., Schnaar, R.L., Esko, J.D., Drickamer, K., Taylor, M.E.: Principles of Glycan Recognition. In: Varki, A., Cummings, R.D., Esko, J.D., Stanley, P., Hart, G.W., Aebi, M., Darvill, A.G., Kinoshita, T., Packer, N.H., Prestegard, J.H., Schnaar, R.L., Seeberger, P.H.: (eds.) Essentials of Glycobiology. pp. 373–385. Cold Spring Harbor Laboratory Press Copyright 2015–2017 by The Consortium of Glycobiology Editors, La Jolla, California. All rights reserved., Cold Spring Harbor (NY) (2015).
17. Schuksz, M., Fuster, M.M., Brown, J.R., Crawford, B.E., Ditto, D.P., Lawrence, R., Glass, C.A., Wang, L., Tor, Y., Esko, J.D.: Surfen, a small molecule antagonist of heparan sulfate. Proc. Natl.

Acad. Sci. USA. **105**(35), 13075–13080 (2008). https://doi.org/10.1073/pnas.0805862105
18. Thacker, B.E., Xu, D., Lawrence, R., Esko, J.D.: Heparan sulfate 3-O-sulfation: a rare modification in search of a function. Matrix Biol. **35**, 60–72 (2014). https://doi.org/10.1016/j.matbio.2013.12.001
19. Lee, M.J.: Heparin inhibits activation of latent transforming growth factor-β1. Pharmacology. **92**(5–6), 238–244 (2013). https://doi.org/10.1159/000355837
20. Lazaridis, D., Leung, S., Kohler, L., Smith, C.H., Kearson, M.L., Eraikhuemen, N.: The Impact of Anticoagulation on COVID-19 (SARS CoV-2) Patient Outcomes: A Systematic Review. J. Pharm. Pract. 08971900211015055 (2021). https://doi.org/10.1177/08971900211015055
21. Tree, J.A., Turnbull, J.E., Buttigieg, K.R., Elmore, M.J., Coombes, N., Hogwood, J., Mycroft-West, C.J., Lima, M.A., Skidmore, M.A., Karlsson, R., Chen, Y.H., Yang, Z., Spalluto, C.M., Staples, K.J., Yates, E.A., Gray, E., Singh, D., Wilkinson, T., Page, C.P., Carroll, M.W.: Unfractionated heparin inhibits live wild type SARS-CoV-2 cell infectivity at therapeutically relevant concentrations. Br. J. Pharmacol. **178**(3), 626–635 (2021). https://doi.org/10.1111/bph.15304
22. Kwon, P.S., Oh, H., Kwon, S.-J., Jin, W., Zhang, F., Fraser, K., Hong, J.J., Linhardt, R.J., Dordick, J.S.: Sulfated polysaccharides effectively inhibit SARS-CoV-2 in vitro. Cell Discovery. **6**(1), 50 (2020). https://doi.org/10.1038/s41421-020-00192-8
23. Tandon, R., Sharp, J.S., Zhang, F., Pomin, V.H., Ashpole, N.M., Mitra, D., McCandless, M.G., Jin, W., Liu, H., Sharma, P., Linhardt, R.J.: Effective Inhibition of SARS-CoV-2 Entry by Heparin and Enoxaparin Derivatives. J. Virol. **95**(3) (2021). https://doi.org/10.1128/jvi.01987-20
24. Xu, D., Esko, J.D.: Demystifying heparan sulfate-protein interactions. Annu. Rev. Biochem. **83**, 129–157 (2014). https://doi.org/10.1146/annurev-biochem-060713-035314
25. Langnau, C., Rohlfing, A.K., Gekeler, S., Günter, M., Pöschel, S., Petersen-Uribe, Á., Jaeger, P., Avdiu, A., Harm, T., Kreisselmeier, K.P., Castor, T., Bakchoul, T., Rath, D., Gawaz, M.P., Autenrieth, S.E., Mueller, K.A.L.: Platelet Activation and Plasma Levels of Furin Are Associated With Prognosis of Patients With Coronary Artery Disease and COVID-19. Arterioscler Thromb Vasc Biol. 2021 Jun;**41**(6):2080-2096. https://doi.org/10.1161/ATVBAHA.120.315698 Epub 2021 Apr 29